Modelling Coupled Motion of Electrons in Quantum Dots with Wetting Layers

R.V.N. Melnik* and M. Willatzen*

* Mads Clausen Institute for Product Innovation
University of Southern Denmark
Grundtvigs Alle 150, DK-6400 Sønderborg, Denmark,
{rmelnik,willatzen}@mci.sdu.dk

ABSTRACT

The influence of wetting-layer states on quantum-dot states and vice-versa is examined numerically employing a one-band model for electrons in the conduction band. This problem corresponds to the case where a few monolayer InAs grown on GaAs(100) oriented substrates leads to self-assembly of quantum dots with wetting layers as is known experimentally. It is shown that the quantum-dot ground state of the combined structure is considerably affected by the presence of the wetting layer, and similarly, wetting-layer states are affected by the presence of the quantum dot. This quantum dot/wetting layer state interference is expected to have an impact on carrier-capture phenomena and operation speeds of electronic and optical devices using quantum dots as active regions.

Keywords: Quantum dots with wetting layers, envelope functions.

1 INTRODUCTION

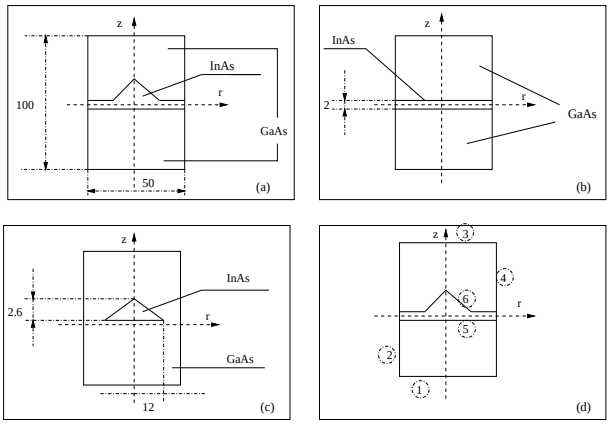

Figure 1: The three geometric configurations considered in the present work: (a) is the full structure with quantum dot and wetting layer, (b) is the isolated wetting layer, and (c) is the isolated conical-shaped quantum dot. The plot shown in (d) defines the boundaries of the computational zone for the full structure. All lengths given in Figure 1 are in nanometers (nm).

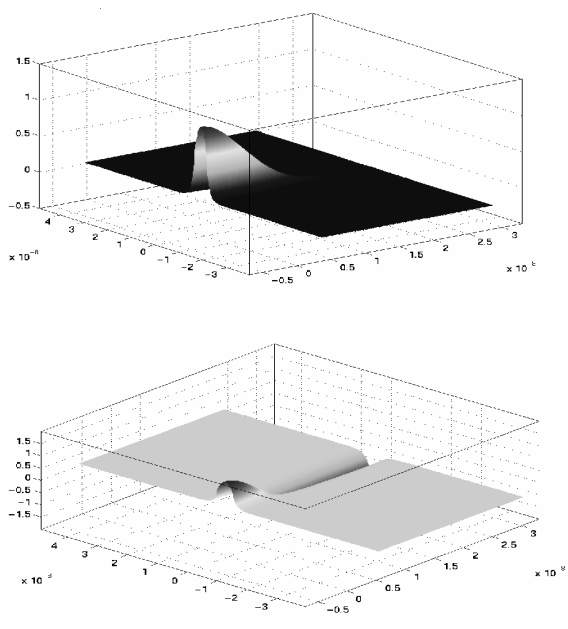

Figure 2: The first two states for the full structure (Figure 1a) in the case where $n = 0$: (a) is the ground state, and (b) is the first excited state.

In recent years, the study of self-assembled quasi-0 dimensional InAs/GaAs heterostructures has attracted considerable theoretical attention [1]–[4] as such structures are expected to form the active regions of next generation electronic and photonic devices. Self-assembled dots meet the requirements that conventional semiconductor processing techniques do not, namely that all physical dimensions can be made smaller than or close to approximately 150 Å which is necessary so as to make them useful in room-temperature applications and to study experimentally fundamental physics of quantum-dot semiconductor structures.

Detailed 8×8 Hamiltonian matrix calculations of electron and hole wavefunctions for states confined to the self-assembled dots have been carried out in, e.g., Refs. [3], [4] including strain, band-mixing, and (in Ref. [3]) piezoelectric effects but the influence of wetting-layer states on dot states and vice versa has been left unexamined so far, even though this study is expected to be of high importance when discussing carrier-capture phe-

nomena from the wetting layer into the (conical) dots, and ultimately to assess the speed of semiconductor devices based on quasi-0 dimensional active regions.

In the present work, one-band model equations for electrons are solved for the multilayer structure consisting of a conical dot and the wetting layer. The main emphasis is given to the discussion of the influence of wetting layer states on quantum dot states and vice versa.

2 THEORY

In the following, a brief account of the effective mass theory for electrons in the case of InAs/GaAs quantum confined heterostructures in 3 dimensions is given. The starting point is the Schrödinger equation in the effective mass approximation

$$-\frac{\hbar^2}{2}\vec{\nabla}\cdot\left(\frac{1}{m_e(\vec{r})}\vec{\nabla}\right)\psi(\vec{r})+V_e(\vec{r})\psi(\vec{r})=E\psi(\vec{r}), \qquad (1)$$

where $\hbar$, $m_e(\vec{r})$, $V_e(\vec{r})$, E, and $\psi(\vec{r})$ are Planck's constant divided by 2π, the position-dependent electron effective mass, the position-dependent band-edge potential energy, the electron energy, and the electron envelope function, respectively. The values of the effective mass m_e and the band-edge potential energy V_e in GaAs and InAs regions are given in Table 1. The values for V_e correspond to those used in Ref. [1]. It will be next assumed that a few monolayer InAs is grown on GaAs(100) oriented substrates such that self-assembly of quantum dots is created and the self-assembled dots take on a conical shape approximating the known experimental shape (see Fig. 1). The distance between individual cones is considered large enough so that electron wavefunctions localized in one cone structure do not overlap in space with electron wavefunctions localized in other cones in the global structure (independence of individual cones). In this approximation, it is possible to calculate bandstructure considering one cone only and the wetting layer.

Parameters	GaAs	InAs
m_e (m_0)	0.067	0.023
V_e (eV)	0	-0.697

Table 1: Conduction-band effective masses and band-edge energies for GaAs and InAs. m_0 is the free-electron mass.

We next introduce cylindrical co-ordinates with the z-axis pointing along the (100) growth direction, r is the in-plane co-ordinate ($r=\sqrt{x^2+y^2}$), and ϕ is the azimuthal angle in the range $[0;2\pi]$. Assuming that $\psi(\vec{r})$ has a separable form in ϕ

$$\psi(\vec{r})=\chi(r,z)\Phi(\phi), \qquad (2)$$

the effective mass equation becomes

$$\Phi(\phi)=\exp(in\phi), \qquad (3)$$

where n is an integer, and

$$-\frac{\hbar^2}{2}\frac{\partial}{\partial z}\left(\frac{1}{m_e(z,r)}\frac{\partial\chi}{\partial z}\right)-\frac{\hbar^2}{2}\frac{1}{r}\frac{\partial}{\partial r}\left(\frac{r}{m_e(z,r)}\frac{\partial\chi}{\partial r}\right)$$
$$+\frac{\hbar^2}{2m_e(z,r)}\frac{n^2}{r^2}\chi(r,z)+V_e(r,z)\chi(r,z)=E\chi(r,z). \qquad (4)$$

Equation (4) is solved for the three different configurations shown in Figs. 1a-1c so as to examine the influence of the few monolayer thick InAs quantum-well (wetting layer) on electron states confined to the dot/cone, and similarly, the influence of the cone structure on InAs wetting-layer electron states. This study is of high importance in relation to carrier capture phenomena, i.e., the process by which electrons are captured from the wetting layer into the quantum dot conical structure [5]. The finite-element-method is employed to solve equation (4) in the weak formulation.

In Figs. 1a-1c, the calculational zones are depicted and spatial dimensions are indicated. In Fig. 1d, the boundaries are numbered. Neumann boundary conditions ($\vec{\nabla}\psi\cdot\vec{n}=0$, where $\vec{n}$ is a normal to the boundary) are imposed on boundary 2 and boundary 4 (Fig. 1d). Far away from the quantum dot, envelope functions must approach asymptotically ordinary quantum-well envelope functions where, of course, the wetting layer is the quantum well. The reason for imposing Neumann conditions on boundaries 2 and 4 now follows as - in the search for solutions - we restrict our attention to those envelope functions for which the in-plane (the plane normal to the z-axis) kinetic energy/wave vector component is zero on boundaries 2 and 4, i.e., $\chi(r,z)=\chi(z)$ on these boundaries. In addition, as we are interested in electron states confined to the InAs regions, Dirichlet boundary conditions ($\psi=0$) are imposed on boundaries 1 and 3. This completes the specification of boundary conditions for our full structure based on a quantum dot with wetting layer.

3 NUMERICAL RESULTS AND DISCUSSIONS

In the following, consider the structure geometries shown in Figs. 1a-1c. Dimensions of the dot are $h=2.6$ nm and $R=12$ nm, where h is the height of the cone (above the wetting layer) and R is the radius of the cone base at the interface between the wetting layer and the cone. The thickness of the wetting layer is assumed to be $L=2.0$ nm, and the dimensions of the computational zone formed by boundaries $(1;3)$ and $(2;4)$ are 50 nm and 100 nm, respectively, in all calculations presented (Figs. 1a-1c). It should be pointed out that convergence were checked for in terms of wavefunctions and

associated energy eigenvalues with respect to lengths of boundaries $1-4$ in all cases.

In Fig. 2a, the ground state envelope wavefunction is shown. It is evident that this wavefunction represents a true quantum-dot state as the wavefunction has its maximum value at the center of the cone and decreases away from the dot center. Observe also that the tail of the wavefunction is larger in the InAs wetting layer as compared to the length of the tail in the GaAs region located near the InAs conical dot. In Fig. 2b, the first excited wavefunction is plotted. Apparently, this state is *not* localized around the dot center since a substantial part of the wavefunction is non-zero everywhere in the wetting layer. This state is a wetting-layer state but the probability of finding the electron near the conical dot is larger than anywhere else. The computed energy eigenvalues for the two states shown in Figs. 2a-2b are -0.4086 eV and -0.3063 eV, respectively.

Next, in Figs. 3a-3d, wavefunction results are shown corresponding to the azimuthal quantum number $n = 1-4$, respectively. It can be seen that as n increases from 1 to 4, the wavefunction gradually becomes less and less confined to the conical dot region. In actual fact, the two states corresponding to $n = 3$ and $n = 4$ are essentially "pure" wetting-layer states in a sense that only a minor part of the wavefunction is located near the conical dot center. It should be pointed out that all wavefunctions corresponding to $n = 1-4$ are zero at the cone center while for $n = 0$, the wavefunction has its maximum value at the center of the conical dot. This behavior is due to the term $\frac{\hbar^2}{2m_e(z,r)}\frac{n^2}{r^2}\chi(r,z)$ in equation (4) and the fact that this term diverges as $r \to 0$ for $n \neq 0$ if $\chi \neq 0$ at the dot center. The energy eigenvalues for the states corresponding to $n = 1, 2, 3,$ and 4 are -0.3289 eV, -0.3059 eV, -0.2949 eV, and -0.2865 eV, respectively.

Finally, it is observed that all wavefunctions shown in Figs. 2a-2b and 3a-3d show ground-state behavior in their z dependence across the quantum-well wetting layer, i.e., the wavefunction has no nodes with respect to the z co-ordinate. This is expected as the wetting-layer thickness is so small that only one quantum-well subband exists.

In Fig. 4a, the ground state wavefunction for the pure wetting layer case is shown. This wavefunction is independent of the r co-ordinate as expected based on symmetry arguments, and agrees with the wavefunction computed using the one-dimensional Ben Daniel-Duke model [6]. The energy of the pure wetting layer ground state is -0.3113 eV which is higher than the ground state energy (-0.4086 eV) in the full structure case as it should be.

In Fig. 4b, the wavefunction for the pure conical-shaped quantum dot is shown. The general shape of this wavefunction is similar to the shape of the ground state wavefunction for the full structure. However, as expected, the tail of the latter wavefunction is longer (and predominantly located in the InAs wetting layer - not in the surrounding GaAs regions), and the probability to find the electron in the dot region is somewhat smaller for the full structure ground state as compared to the ground state for the pure quantum-dot case. The ground state energy is higher in the pure quantum-dot case (-0.2175 eV) as compared to the ground state energy (-0.4086 eV) for the full structure (i.e., quantum dot and wetting layer) case. Again, this is expected, since the amount of GaAs present in the pure quantum-dot case is higher than for the full structure keeping in mind that the conduction band-edge energy of GaAs is higher than that of InAs.

4 Conclusions

The influence of wetting-layer states on conical-shaped quantum dot states and vice versa is examined theoretically for electrons using a one-band model. The model analyzed corresponds to the case where a few monolayer InAs is grown on GaAs(100) and self-assembly of quantum dots takes place as it is known experimentally. This problem is important when assessing carrier scattering processes in general involving wetting-layer states and confined quantum-dot states including carrier-capture phenomena. In particular, the operation speed of next generation electronic and optical devices based on quantum-dot active regions strongly relies on obtaining high carrier capture rates from the wetting layer into the quantum dot regions.

Future work will include calculations of electron and hole states by using the 8×8 Luttinger-Kohn and Pikus-Bir strain Hamiltonians for the full structure consisting of quantum dot and wetting layer. This will allow us to calculate and examine optoelectronic properties of structures based on quantum dots with wetting layers.

REFERENCES

[1] J. Y. Marzin and G. Bastard, Solid State Comm., 92, 437–442, 1994.

[2] S. Li, J. Xia, Z. L. Yuan, Z. Y. Xu, W. Ge, X. R. Wang, Y. Wang, J. Wang, and L. L. Chang, Phys. Rev. B, 54, 11575–11581, 1996.

[3] O. Stier, M. Grundmann, and D. Bimberg, Phys. Rev. B, 59, 5688–5701, 1999.

[4] H. Jiang and J. Singh, IEEE J. Quant. Electron., 34, 1188–1196, 1998.

[5] A. V. Uskov, A.-P. Jauho, B. Tromborg, J. Mørk, and R. Lang, Phys. Rev. Lett., 85, 1516–1519, 2000.

[6] G. Bastard, "Wave Mechanics Applied to Semiconductor Heterostructures", Halsted Press, 1988.

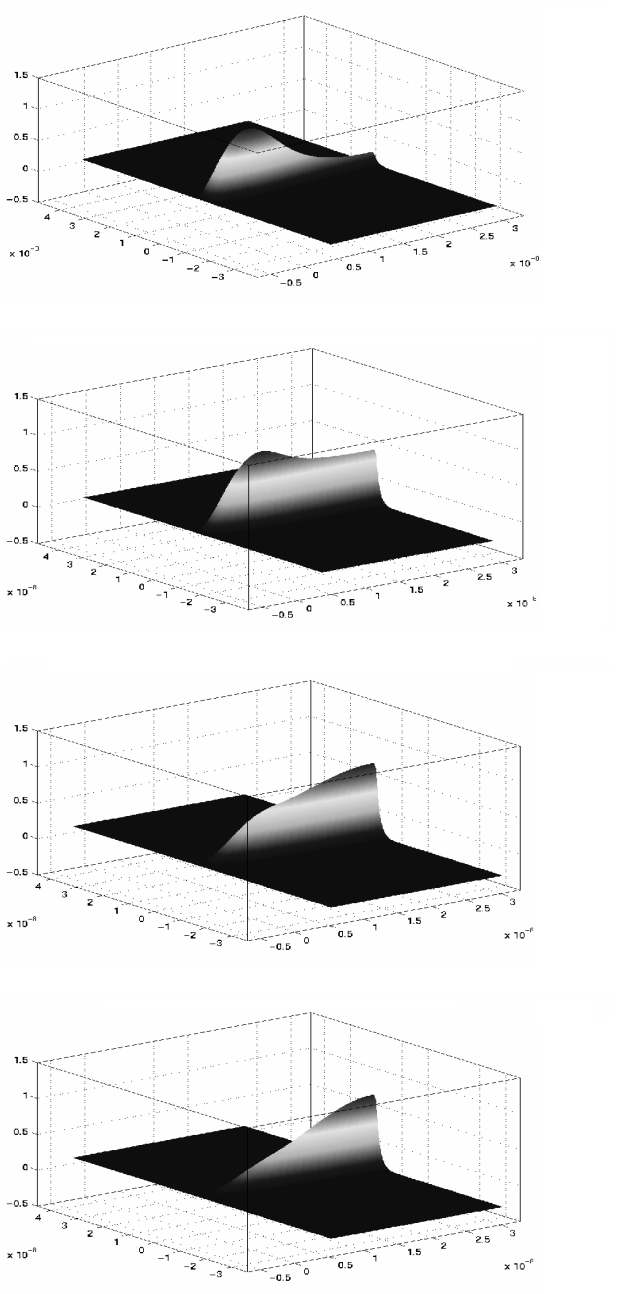

Figure 3: The ground state for the full structure (Figure 1a) in the cases: (a) $n = 1$, (b) $n = 2$, (c) $n = 3$, and (d) $n = 4$.

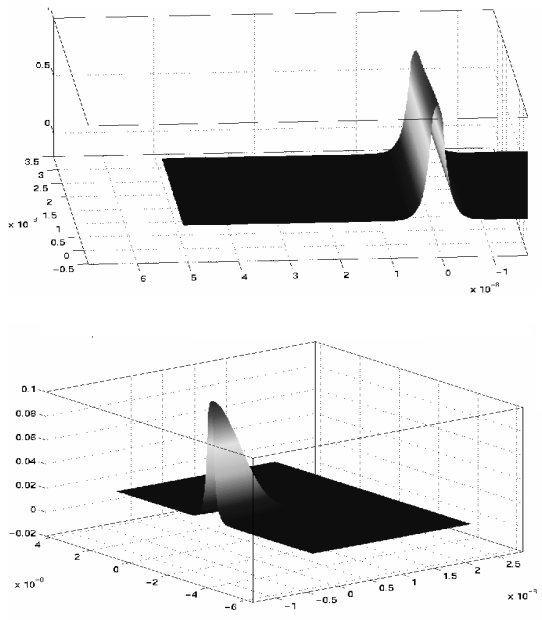

Figure 4: The ground state for: (a) the pure wetting layer shown in Figure 1b, and (b) the conical-shaped quantum dot shown in Figure 1c.